Conference on Modelling Fluid Flow (CMFF'25)
The 19th International Conference on Fluid Flow Technologies
Budapest, Hungary, August 26 - August 29, 2025

DETAILED CHARACTERISATION OF PORE STRUCTURE AND TRANSPORT PROPERTIES OF BIOMASS PARTICLES DURING PYROLYSIS

N. Zhan[1,3], E. Liu[1], A. Dernbecher[2], N. Vorhauer-Huget[1], R. Wu[3], A. Dieguez-Alonso[2], A. Kharaghani[1*]

[1]Chair of Thermal Process Engineering, University Magdeburg, Universitätsplatz 2, 39106 Magdeburg, Germany. E-Mail: reza.kharaghani@ovgu.de
[2]Laboratory of Transport Processes, Faculty Biochemical and Chemical Engineering, TU Dortmund University, Emil-Figge-Str. 68, 44227 Dortmund, Germany
[3]School of Mechanical Engineering, Shanghai Jiao Tong University, Shanghai 200240, China

ABSTRACT

This study presents an advanced investigation into the dynamic evolution of pore structures in woody biomass during pyrolysis, focusing on the critical roles of structural heterogeneity and anisotropy. Building on earlier work that used X-ray micro-computed tomography (μ-CT) to analyse beech wood particles pyrolysed at various temperatures, we extended the analysis to track how structure and transport properties evolve throughout the pyrolysis process. Using the μ-CT images, we developed an equivalent pore network model (PNM) to simulate changes in permeability and gas flow behaviour over time. By segmenting the biomass into representative elementary volumes (REVs), the model accurately captured localised variations in porosity and permeability across the entire particle. Simulation results show that as the pyrolysis temperature increases, the anisotropic transport properties first decrease and then rise sharply, primarily due to directional pore expansion and the evolution of connectivity patterns. This integrated modelling framework offers deeper insights into structure-property relationships during biomass pyrolysis and supports the design and optimisation of gas transport processes in thermochemically evolving, thermally-thick porous particles.

Keywords: Anisotropic pores, biomass, heterogeneous pore structure, pyrolysis, pore morphology evolution, pore network modelling

NOMENCLATURE

φ	[°]	azimuth angle
θ	[°]	elevation angle
K	[m^2]	local permeability
ε	[-]	local porosity
r	[m]	radial distance
L_r	[-]	radial layer

Abbreviations

PNM	pore network model
OED	Omnidirectional Euclidean Distance
REV	representative elementary volume
μ-CT	X-ray micro-computed tomography

1. INTRODUCTION

Biomass pyrolysis, a promising thermochemical conversion process, has gained considerable attention for its potential to produce renewable fuels, valuable chemicals, and biochar [1]. Among the various biomass resources, woody biomass is particularly favoured due to its abundant availability, carbon-neutral profile, and relatively high energy density [2]. However, predicting pyrolysis behaviour remains challenging due to structural heterogeneity and anisotropy inherent in woody biomass. These complexities are further compounded in thermally-thick particles, where internal temperature and transport gradients significantly influence conversion pathways.

During pyrolysis, complex physicochemical transformations drive the decomposition of biomass components and the concurrent evolution of a porous structure within the particle. These transformations critically affect heat and mass transfer processes. Conventional models often oversimplify biomass as a homogeneous porous medium, neglecting the anisotropic nature of wood and the dynamic evolution of its pore network [3]. Consequently, there is a growing demand for advanced modelling frameworks that can capture the large-scale, heterogeneous, and dynamic characteristics of biomass pyrolysis.

Pore network modelling (PNM) has emerged as an effective tool to simulate transport phenomena in

complex pore structures [4,5]. In PNM, the biomass structure is abstracted into a discrete network of pores (nodes) and throats (bonds), where large voids are considered pore bodies, and the narrow connections between them are throats. Accurate construction of such networks requires high-fidelity imaging data. Advances in X-ray micro-computed tomography (μ-CT) have enabled the acquisition of high-resolution 3D images of biomass at various stages of pyrolysis, providing the structural basis for extracting realistic pore networks [6,7]. These images allow detailed characterisation of pore morphology, connectivity, and their evolution under thermal stresses.

In pyrolysing woody biomass, structural anisotropy significantly influences transport properties. However, extracting anisotropic pore structures with high fidelity remains a key challenge. To address this, we previously developed the Omnidirectional Euclidean Distance-based (OED-based) method, a pore-network extraction algorithm developed to accurately capture elongated and directionally aligned pores [8,9]. Incorporating such anisotropy into PNMs significantly improves the predictive capability of the model, especially when validated against experimental μ-CT data.

A critical aspect of pyrolysis is the dynamic evolution of pore connectivity, which governs intra-particle gas flow and the release of volatile compounds. As temperature increases, pores expand, elongate, or collapse, leading to significant changes in local permeability. These morphological changes often occur preferentially along specific directions, giving rise to anisotropic transport behaviour. This directional permeability is especially relevant in thermally-thick particles, where heterogenous temperature profiles and reaction rates drive localised structural changes. However, accurately modelling these effects is challenging due to the interplay between pore network dynamics and reactive gas flow. One major challenge in modelling biomass pyrolysis is accounting for the anisotropic transport properties resulting from the irregular and evolving pore network. Anisotropy in biomass is inherently linked to its hierarchical structure, where different wood components (e.g., vessels, fibres, and rays) contribute differently to permeability and thermal conductivity [10]. During pyrolysis, the decomposition of these components further modifies the pore network, leading to dynamic changes in anisotropic behaviour.

In addition to anisotropy, biomass heterogeneity further complicates pyrolysis modelling. Variability in pore size, orientation, and connectivity introduces localised differences in gas permeability and thermal diffusivity [11]. This is particularly evident in the outer layers of particles, which experience more rapid thermal and structural evolution. The resulting pressure gradients and flow pathways can significantly affect char yield and volatile escape.

Despite recent advances in PNM-based modelling, limitations remain in capturing the full temporal evolution of pore networks during pyrolysis. Since the decomposition of biomass components occurs at varying rates and temperatures, it is essential to update of the pore network dynamically to reflect ongoing structural changes. Additionally, accurately modelling the feedback between evolving structure and transport properties, particularly pressure-driven gas flow, requires a meticulous integration of experimental data with simulation frameworks.

This study aims to bridge the gap between pore-scale dynamics and macro-scale pyrolysis modelling by constructing deformable pore network models based on high-resolution μ-CT images of woody biomass. Focusing on thermally-thick particles, the model incorporates both anisotropic and heterogeneous features to capture the evolution of transport-relevant properties during pyrolysis. By segmenting particles into representative elementary volumes (REVs), we quantify local variations in porosity and permeability and explore how structural evolution governs gas transport characteristics. Ultimately, this work provides a comprehensive framework for understanding the structure-property-performance relationships in biomass pyrolysis and contributes to optimisation of thermal conversion technologies.

2. METHODS

2.1. Experiments and Characterisation

Beech wood spheres (10 mm diameter) were pyrolysed in a tubular reactor under a nitrogen (N_2) atmosphere (Fig. 1a). Preheated N_2 passed through an inert porous bed before contacting the particles. The heating rate was 10 °C/min, with final temperatures between 100 °C and 500 °C, held for about 30 minutes. Three spheres were pyrolysed simultaneously in a small basket hung from a scale for mass monitoring. Due to the small size of the particles relative to the reactor, heating conditions were considered uniform. One particle was drilled for internal temperature measurement, a second was used for μ-CT imaging, and the third for physic-chemical analysis. μ-CT imaging was performed on the same particle at different pyrolysis stages. After each treatment, the particle was cooled, analysed and reheated to the next temperature. Figure 1b presents photographs of wood particles at different pyrolysis stages. We selected four representative stages, corresponding to samples treated at 100°C, 300°C, 400°C, and 500°C, which are denoted as WP100, WP300, WP400, and WP500, respectively. Note that the sample treated at 200°C was excluded from this analysis, as its characteristics were observed to be largely similar to those of the 100°C sample.

The structural characterisation of wood and char samples treated at different temperatures was

performed using X-ray microcomputed tomography (μ-CT) with a Proton CT alpha system (Proton X-ray GmbH, Germany). The scans were conducted at 100 kV, 30 mA, and 2000 ms exposure time, with 1200 projections (3 radiographs per projection) and a voxel size of 5.9 μm. The sample-to-detector distance was 630 mm, allowing for a resolution sufficient to detect pores larger than 15 μm, thereby capturing only macropores. Similar resolution limits for μ-CT have been reported in the literature [12].

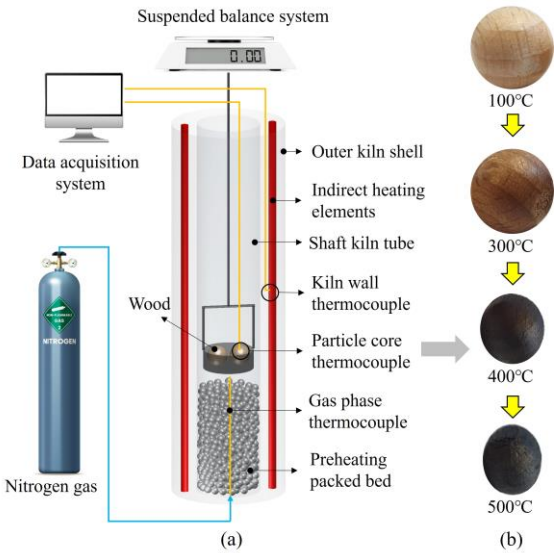

Fig. 1 Experimental setup: Tubular reactor used for pyrolysis of beech wood spheres at varying temperatures.

2.2. Pore Network Extraction

To accurately model the pore structure of beech wood particles, a PNM was constructed based on the extracted real pore geometry, capturing both the geometric and topological characteristics of the porous medium. This model not only preserves the anisotropic features of the pore structure but also accounts for the heterogeneous distribution of structural parameters and transport properties across the entire particle.

The pore network extraction was performed using the OED-based method, as described in our previous study [8,9]. The process involves identifying anchored void voxels on the boundary surfaces and calculating the OED for each void voxel to establish a hierarchical arrangement. Using the omnidirectional distance order homotopic thinning (ODOHT) algorithm, the medial axes (MAs) are extracted, and pore and throat positions are identified. The resulting pore network is represented as a graph where nodes correspond to pore and throat centres, and bonds capture the connectivity of the porous structure. To efficiently handle large-scale CT images (1936×1936×1383 voxels, see the left side of Fig. 2a), the domain was decomposed into subdomains, enabling parallel processing for network extraction. The partial MAs from each subdomain were then merged to reconstruct the complete pore network, maintaining both computational efficiency and accuracy. The extraction results of the entire wood particle are shown on the right side of Fig. 2a.

To characterise the anisotropy of the pore structure, ellipsoids were fitted to individual pores, with each pore's orientation defined by the semi-principal axes of the fitted ellipsoid. To visualise the directional distribution, the semi-major axis orientation was converted into elevation, θ_p, and azimuth, φ_p, angles (Fig. 2b). By calculating the angle between the semi-major axis and a reference direction, the frequency of orientation vectors within a 10° range was determined. This approach captures the inherent anisotropy of the wood pore structure effectively.

To evaluate heterogeneity, the entire particle was divided into multiple representative elementary volumes (REVs) based on a polar coordinate grid (Fig. 2c). For each REV, the sub pore networks were obtained and single-phase pressure field simulations were performed to calculate intrinsic permeability. The radial distribution of pressure was then calculated (Fig. 2c). This multi-scale approach ensures a comprehensive representation of both anisotropy and heterogeneity within the pore network model, facilitating the analysis of flow transport processes in porous wood structures.

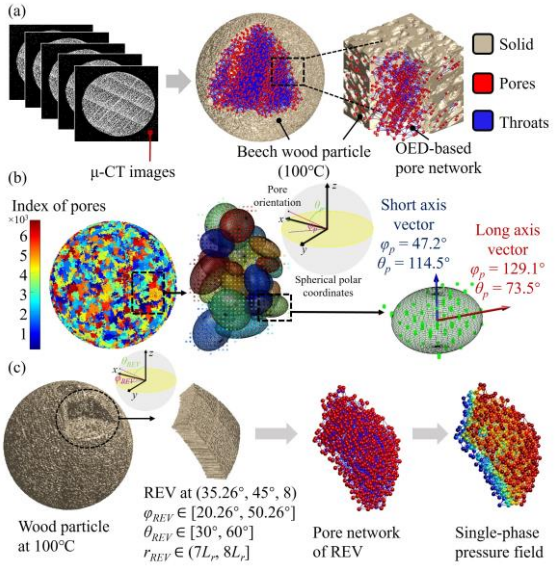

Fig. 2 (a) Large-scale pore network extraction from μ-CT images of beech wood particle. (b) Discretisation of pore bodies using point cloud data with ellipsoids fitted to represent the pore geometry. (c) The segmentation of wood particles into multiple REVs using a polar coordinate grid and the radial pressure distribution of the REV.

2.3. Pore Network Simulations

During pyrolysis, the evolution of the solid phase can be effectively represented using a

deformable pore network model. This model integrates the structural changes in the pore network as the wood particles undergo thermal decomposition. Specifically, pore bodies and throats are linked with adjacent solid elements, which gradually diminish as pyrolysis progresses, as shown in Fig. 3. As the solid elements on the pore surfaces reduce, the pore size increases until the solid elements at the surface completely vanish. At this stage, external pores and throats are removed, and new boundary pore-throat connections are identified, as illustrated in Fig. 3a. Figure 3b depicts the overall process by which the deformable pore network model captures the evolution of the solid phase.

To simulate the pyrolysis flow process, we construct deformable pore networks based on images obtained from wood particles at different temperatures during pyrolysis. It should be noted that the current deformable PNM does not incorporate the reaction kinetics of wood pyrolysis, which will be addressed in future work. In this study, the primary focus is on the structural evolution of biomass pore networks during pyrolysis, and all structural changes are derived directly from experimental CT image data. By quantifying the loss of solid mass, we calculate the gas flow rate generated during pyrolysis. This calculated flow rate is then incorporated into the deformable pore network model to simulate gas transport through the evolving porous structure. This approach enables an accurate representation of the dynamic changes occurring within the wood particle during pyrolysis, thereby enhancing the predictive accuracy of multiphase flow behaviour in the context of thermal decomposition.

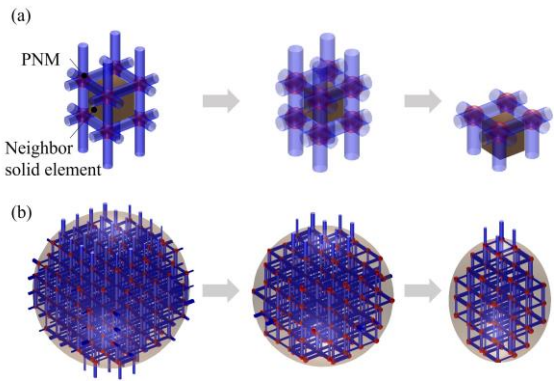

Fig. 3 Representation of the evolution of the solid phase during pyrolysis process within the framework of pore network modelling. (a) The reduction and disappearance of solid elements result in the expansion and eventual removal of neighbour pores and throats, (b) a deformable pore network captures the evolution of the pore structure throughout the pyrolysis process.

3. EVALUATION AND ANALYSIS

3.1. Structure Analysis and Anisotropy

The extraction algorithm described in Sec. 2.2 was applied to the original μ-CT images of wood particles obtained at different pyrolysis temperatures. This approach enabled the reconstruction of pore network models corresponding to each pyrolysis condition. The key structural parameters extracted from these PNMs are summarised in Table 1.

Table 1. Structural parameters of extracted PNMs of wood particles at different temperatures.

Sample	Domain (voxels × voxels × voxels)	Pore number	Throat number	porosity
WP100	(1384×1384×1384)	41803	227339	0.473
WP300	(1264×1000×1320)	30599	181296	0.456
WP400	(1040×960×1280)	21458	125892	0.545
WP500	(920×744×1080)	10362	63386	0.578

Figure 4 illustrates the evolution of wood pore structures at different pyrolysis temperatures: (a) 100°C, (b) 300°C, (c) 400°C and (d) 500°C. Each row in the figure has three parts. The first shows the OED maps of reconstructed wood structure based on image data and matches the actual structures shown in Fig. 1b. The second and third parts show the azimuth and elevation angles of the pores, based on fitted ellipsoids, as descripted in Fig. 2b.

From the first column, one can see that as the temperature rises, the amount of solid wood decreases (see also Fig. 1b). This is expected, as more material breaks down and volatile gases are released during pyrolysis. Even as the structure changes, the pores remain strongly oriented in one main direction – a clear sign of anisotropy. This effect is evident at all temperatures, especially at 500°C.

To quantitative analysis this pore structure anisotropy, we fitted ellipsoids to the pore bodies (as shown earlier in Fig. 2b). Each ellipsoid's major axis points in the direction of the largest pore dimension, helping us to define the main pore orientation. The azimuth and elevation angle distributions in the second and third columns show that pore orientations are strongly clustered rather than uniformly distributed. The clustering in the azimuthal distribution initially decreases with increasing pyrolysis temperature but then increases significantly, becoming particularly pronounced at 500°C. The elevation angle distribution also exhibits a concentrated pattern, further marking the anisotropic character of the pore network.

The alignment between the OED map and the orientation angle distributions demonstrates that the proposed ellipsoid fitting method accurately captures the anisotropic characteristics of the pore structure. This ability to quantitatively describe anisotropy isessential for understanding the relationship

between structural evolution and transport properties of the wood during pyrolysis. Since material transport properties are inherently influenced by structural orientation, the identified anisotropy directly affects gas flow and diffusion, which will be further analysed in subsequent sections.

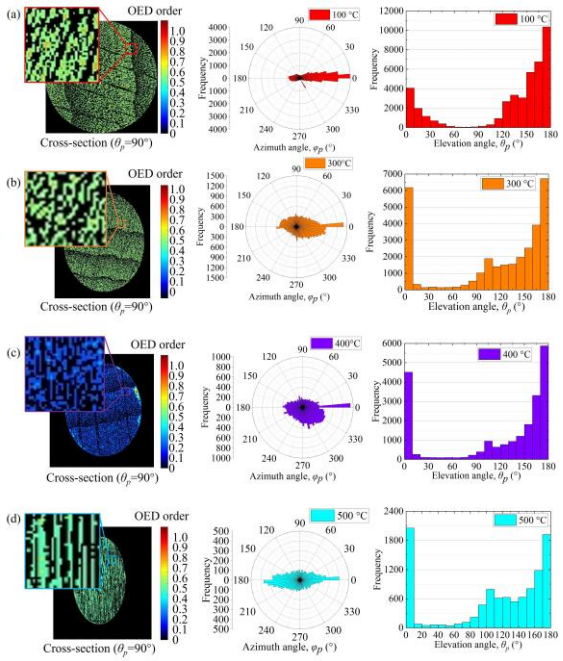

Fig. 4 Pore orientation analysis of wood particles at different temperatures: (a) 100°C, (b) 300°C, (c) 400°C, and (d) 500°C. The first column shows the sectional OED map; the second and third columns display the azimuth and elevation angle distributions of the fitted ellipsoids representing pore bodies, respectively.

3.2. Spatial Heterogeneity of Porosity and Permeability

To fully understand the structure of wood particles, two key aspects must be considered: anisotropy and heterogeneity. The previous section addressed anisotropy, highlighting the directional dependence of wood properties. In this section, the focus shifts to heterogeneity, which refers to spatial variations in material properties.

Wood is not a uniform substance. It consists of distinct components such as fibres and vessels that are unevenly distributed throughout the material. These structural differences cause complex variations at the microscopic level. Therefore, a comprehensive analysis must account for both the directional and spatial variability of wood. This section investigates how structural and transport properties vary across different regions of the particle.

To quantify heterogeneity, each wood particle is divided into representative elementary volumes (REVs) using a polar coordinate system (φ_{REV}, θ_{REV}, r_{REV}), as shown in Fig. 2c. Since the original wood particles are approximately spherical, the domain for heterogeneity analysis at all temperatures is based on the initial spherical particle region. The segmentation consists of 36 divisions in the azimuthal angle, φ_{REV}, 18 in the elevation angle, θ_{REV}, and 5 layers in radial distance, r_{REV}. As pyrolysis progresses, REVs where the solid phase disappears correspondingly increase porosity. If the remaining solid fraction in an REV becomes too low, its permeability will not be calculated. These details will be discussed further in the following sections. This framework allows for a detailed spatial analysis of heterogeneity across the entire particle.

From each REV, a sub-PNM is generated, and key local properties – such as porosity (ε_{REV}) and normalized permeability (K_{REV}) – are calculated. These are presented in Fig. 5 (ε_{REV}) and Fig. 6 (K_{REV}), which show the spatial distribution of these parameters within individual REVs in three-dimensional coordinates. The left columns of both figures show the full REV-level distributions, where part of the volume has been virtually removed to expose the internal radial layers. The right columns focus on radial layers 2 to 5, omitting layer 1 due to its irregular and non-representative patterns.

The porosity distributions under different thermal conditions reveal key insights. At 100°C, porosity remains relatively uniform throughout most of the particle, except in regions aligned with wood grain structures – dense, annular features show distinctly lower porosity values. At 300°C, highly porous zones with porosity values close to 1 begin to appear in the outermost radial layers (layers 4 and 5). These zones indicate complete pyrolysis within affected REVs, where solid matter has fully decomposed. In contrast, inner layers at this temperature retain porosity patterns similar to those observed at 100°C, though with a slight increase in average porosity.

By 400°C, the volume and continuity of fully pyrolysed regions grow substantially, forming larger and more connected high-porosity zones. At 500°C, the outer two radial layers become entirely pyrolysed, forming continuous, highly porous regions. This transformation marks a significant structural collapse, with a notable reduction in the overall particle volume due to extensive thermal degradation.

Permeability distributions were also analysed and are presented in Figs. 7 and 8. The values shown represent normalised permeability, defined as the single-phase intrinsic permeability of each REV normalised by the maximum permeability among all REVs. To ensure consistency and meaningful interpretation, REVs with porosity greater than 0.9 were excluded from the analysis, as these REVs are considered fully pyrolysed and no longer possess a well-defined porous structure that contributes to flow resistance.

Overall, regions with higher porosity tend to exhibit higher normalized permeability.

Additionally, permeability values are notably higher near both ends of the z-axis. This observation indicates that permeability is influenced not only by porosity but also by the directional organisation of the pore structure. The spatial distribution reflects the combined effects of porosity and anisotropy on fluid transport within the material.

These findings suggest that transport properties in pyrolysed wood particles are controlled by both the extent of thermal decomposition and the orientation of the internal pore structure. Quantitative retails of porosity and permeability distributions are provided in Fig. 7 and 8 for reference.

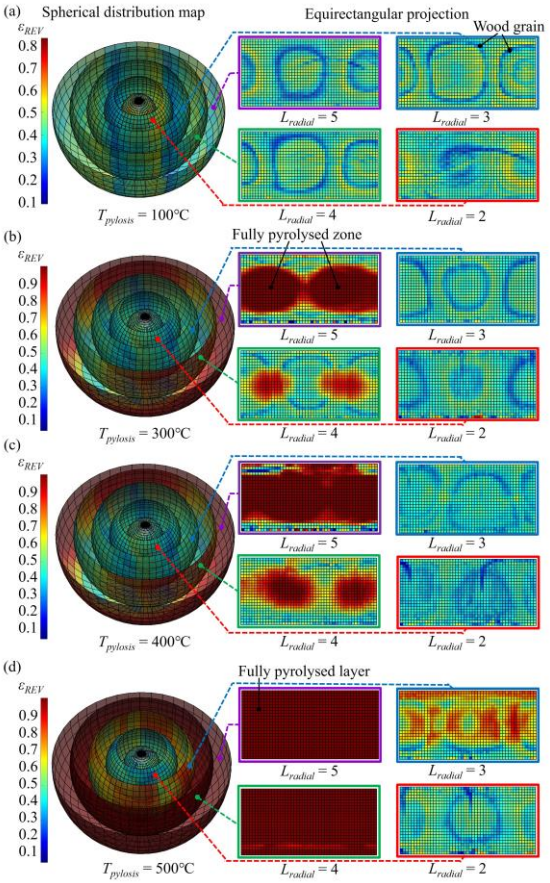

Fig. 5 Porosity distribution of wood particles at different temperatures: (a) 100°C, (b) 300°C, (c) 400°C and (d) 500°C.

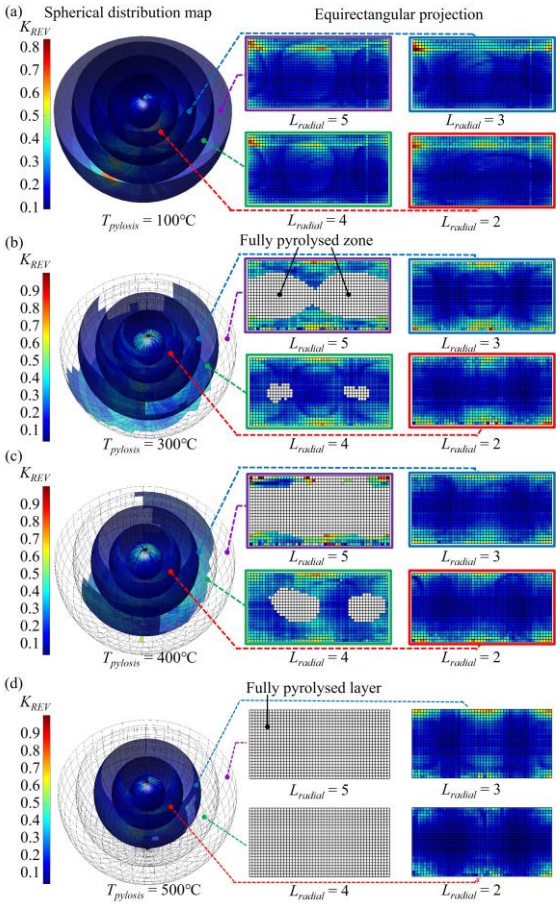

Fig. 6 Normalised permeability distribution of wood particles at different temperatures: (a) 100°C, (b) 300°C, (c) 400°C and (d) 500°C.

Figures 7 and 8 expand on this by showing the angular distributions of porosity and normalised permeability as a function of azimuth and elevation angles. Each curve represents the average value across all REVs within each angular segment, offering a directional perspective on the data. The porosity distribution shows lower values along the wood grain and near-complete voids in fully pyrolysed regions, consistent with earlier spatial observations. In contrast, the normalised permeability distribution exhibits a more complex, multimodal pattern, shaped by both porosity and the anisotropic organisation of the pore network.

These angular trends further underscore the strong directional dependence of transport behaviour in thermally decomposed wood.

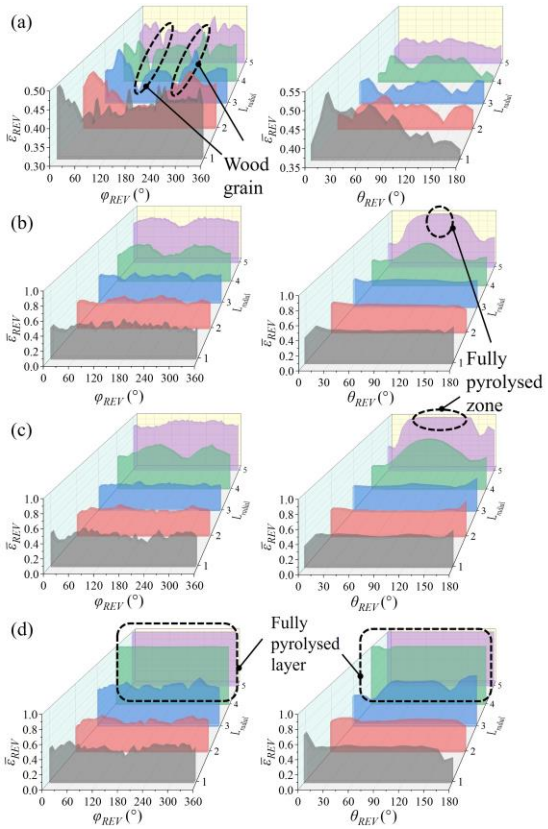

Fig. 7 Porosity distribution in φ_{REV} and θ_{REV} directions of wood particles at different temperatures: (a) 100°C, (b) 300°C, (c) 400°C and (d) 500°C.

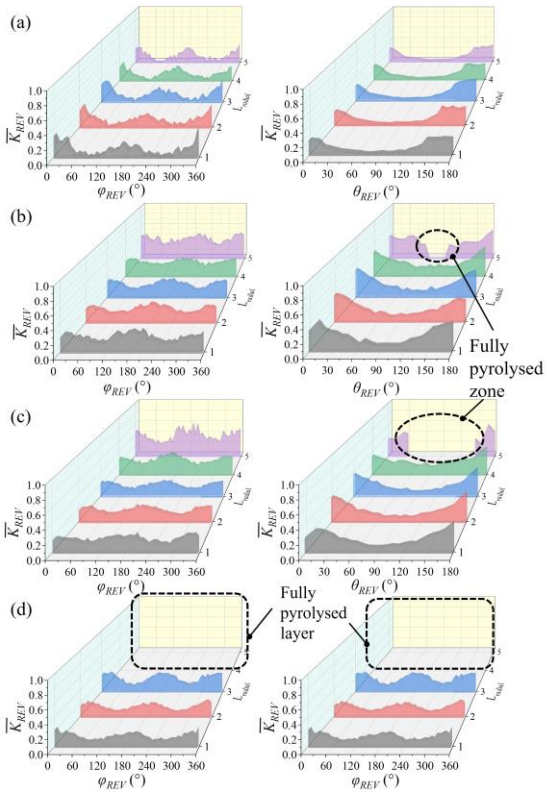

Fig. 8 Permeability distribution in φ_{REV} and θ_{REV} directions of wood particles at different temperatures: (a) 100°C, (b) 300°C, (c) 400°C and (d) 500°C.

3.3. Spatially Resolved Pressure Fields and Transport Behaviour during Pyrolysis

As pyrolysis progresses, the solid phase within the wood particles decomposes, resulting in gradual pore expansion. In the outermost regions, pores grow until they disappear and are replaced by newly formed pores further inward (Fig. 3a). This dynamic is modelled by converting solid mass loss into gas generation, followed by transport simulation throughout the pyrolysis process.

Figure 9 presents the simulated pressure fields at 100 ° C, 300 ° C, 400 ° C, and 500 ° C. Pressure propagates more efficiently along the x-direction than the y-direction, indicating strong anisotropy. This directional behaviour corresponds to the pore orientation (Fig. 4) and permeability distributions (Fig. 6). Areas with larger, better-aligned pores exhibit lower flow resistance and faster pressure transmission.

These findings are consistent with earlier studies on anisotropic porous media undergoing thermal decomposition, where directional pore growth and preferential gas flow were also observed. Our results further emphasize the need to accurately capture evolving pore structure in order to model transport processes in reactive porous materials.

In future work, we will compare REV-based simulation results with those obtained from homogenized models and full-scale pore network modelling. This comparison will include not only pressure distribution but also other key transport metrics, providing a more comprehensive evaluation of model performance and predictive capability.

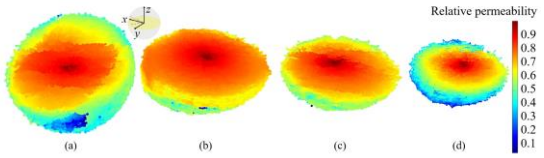

Fig. 9 Simulated pressure fields in the PNM model of wood particles at different pyrolysis temperatures: (a) 100°C, (b) 300°C, (c) 400°C, and (d) 500°C. The pressure distribution demonstrates increasing anisotropy with temperature, consistent with the evolving pore structure and permeability.

4. SUMMARY

Biomass pyrolysis is a critical thermochemical process for converting renewable feedstocks into fuels, chemicals, and biochar. Among biomass resources, woody biomass offers significant advantages due to its availability and carbon-neutral profile. However, accurately predicting pyrolysis behaviour remains challenging because of the

complex, evolving pore structures within the biomass during thermal decomposition.

This study investigates the structural and transport property evolution in beech wood particles under pyrolysis using PNM derived from high-resolution μ-CT images. The extracted networks at different temperatures capture key features such as pore growth, anisotropic expansion, and regional variation in porosity and permeability. Quantitative structural analysis based on fitted ellipsoids reveals that the pore orientation becomes increasingly anisotropic as temperature rises, especially at 500°C. The azimuthal and elevation angle distributions confirm strong directional clustering, indicating a consistent alignment of pores along preferred axes.

To assess spatial heterogeneity, each wood particle was segmented into representative elementary volumes (REVs) in a polar coordinate system. This allows for local evaluation of porosity and permeability. The results demonstrate clear radial and angular heterogeneity. Outer layers undergo full pyrolysis at higher temperatures, resulting in porosity values close to 1 and structural collapse. In contrast, inner layers retain partial solid structure. Permeability distributions are more complex, influenced by both porosity and pore orientation. Higher permeability is observed not only in high-porosity zones but also in directions aligned with major pore axes. Simulated pressure fields at multiple pyrolysis stages show increasing anisotropy in fluid transport. Pressure propagates more efficiently along the primary pore alignment, confirming the influence of both structural orientation and decomposition extent. These trends are consistent with earlier findings in thermally decomposing porous media.

Overall, this study provides a detailed spatially resolved analysis of pore structure and transport property evolution during wood pyrolysis. By combining local REV-based characterization with PNM simulation, we bridge the gap between microstructural changes and macroscopic transport behaviour. Future work will compare REV-based simulation outcomes with homogenized models and full-network computations. The evaluation will go beyond pressure fields to include comprehensive transport metrics, improving the accuracy and reliability of pyrolysis modelling frameworks for biomass conversion applications.

ACKNOWLEDGEMENTS

Funded by the Deutsche Forschungsgemeinschaft (DFG, German Research Foundation) – Project-ID 422037413 – TRR 287.

REFERENCES

[1] Lopez, G., Keiner, D., Fasihi, M., Koiranen, T., Breyer, C., 2023, " From fossil to green chemicals: sustainable pathways and new carbon feedstocks for the global chemical industry", *Energy & Environmental Science*, Vol. 16, pp. 2879-2909.

[2] Vilas-Boas, A. C. M., Tarelho, L. A. C., Oliveira, H. S. M., Silva, F. G. C. S., Pio, D. T., Matos, M. A. A., 2024, "Valorisation of residual biomass by pyrolysis: influence of process conditions on products", *Sustainable Energy & Fuels*, Vol. 8, pp. 379-396.

[3] Bermúdez, C. A., Porteiro, J., Varela, L. G., Chapela, S., Patiño, D., 2020, "Three-dimensional CFD simulation of a large-scale grate-fired biomass furnace", *Fuel Processing Technology*, Vol. 198, pp. 106219.

[4] Jiang, Z., Wu, K., Couples, G., Van Dijke, M. I. J., Sorbie, K. S., Ma, J., 2007, "Efficient extraction of networks from three‐dimensional porous media", *Water resources research*, Vol. 43, pp. 12.

[5] Gostick, J. T., 2017, "Versatile and efficient pore network extraction method using marker-based watershed segmentation", *Physical Review E*, Vol. 96, pp. 023307.

[6] Edeh, I. G., Masek, O., Fusseis, F., 2023, "4D structural changes and pore network model of biomass during pyrolysis", *Scientific Reports*, Vol. 13, pp. 22863.

[7] Srocke, F., Han, L., Dutilleul, P., Xiao, X., Smith, D. L., Mašek, O., 2021, "Synchrotron X-ray microtomography and multifractal analysis for the characterization of pore structure and distribution in softwood pellet biochar", *Biochar*, Vol. 96, pp. 671-686.

[8] Zhan, N., Wu, R., Tsotsas, E., Kharaghani, A., 2022, "Proposal for extraction of pore networks with pores of high aspect ratios", *Physical Review Fluids*, Vol. 7, pp. 014304.

[9] Zhan, N., Wang, Y., Lu, X., Wu, R., Kharaghani, A., 2024, "Pore-corner networks unveiled: Extraction and interactions in porous media", *Physical Review Fluids*, Vol. 9, pp. 014303.

[10] Yapici, F., Ozcifci, A., Esen, R., Kurt, S., 2011, "The effect of grain angle and species on thermal conductivity of some selected wood species", *BioResources*, Vol. 6, pp. 2757-2762.

[11] Pecha, M. B., Thornburg, N. E., Peterson, C. A., Crowley, M. F., Gao, X., Lu, L., Wiggins, G., Brown, R. C., Ciesielski, P. N., 2021, "Impacts of anisotropic porosity on heat transfer and off-gassing during biomass pyrolysis", *BioResources*, Vol. 35, pp. 20131-20141.